Solar-Heating Boosted Catalytic Reduction of CO_2 under Full Solar Spectrum

Hongjia Wang,[†,‡] Yanjie Wang,[†] Lingju Guo,[†] Xuehua Zhang,[†] Caue Ribeiro,[§,#] and Tao He[†,‡]*

[†]CAS Laboratory of Nanosystem and Hierarchical Fabrication, CAS Center for Excellence in Nanoscience, National Center for Nanoscience and Technology, Beijing 100190, China

[‡]University of Chinese Academy of Sciences, Beijing 100049, China

[§]National Nanotechnology Laboratory for Agribusiness, Embrapa Instrumentation, 13561-206, São Carlos – SP, Brazil

[#]Forschungszentrum Jülich GmbH – Institute of Energy and Climate Research – IEK-3 / Electrochemical Process Engineering, Jülich 52425, Germany

*To whom correspondence should be addressed; Tel: +86-10-82545655; Fax: +86-10-62656765

E-mail: het@nanoctr.cn

ABSTRACT

Catalytic converting CO_2 into fuels with the help of solar energy is regarded as 'dream reaction', as both energy crisis and environmental issue can be mitigated simultaneously. However, it is still suffering from low efficiency due to narrow solar-spectrum utilization and sluggish heterogeneous reaction kinetics. In this work, we demonstrate that catalytic reduction of CO_2 can be achieved over Au nanoparticles (NPs) deposited rutile under full solar-spectrum irradiation. We found that UV and visible light can activate the reaction, and the heat from IR light and local surface-plasmon resonance relaxation of Au NPs can boost the reaction kinetically. The apparent activation energy is determined experimentally and is used to explain the superior catalytic activity of Au/rutile to rutile in a kinetic way. We also found the photo-thermal synergy in the Au/rutile system. We

envision that this work may facilitate understanding the kinetics of CO_2 reduction and developing feasible catalytic systems with full solar spectrum utilization for real artificial photosynthesis.

KEYWORDS: CO_2 reduction; apparent activation energy; reaction kinetics; solar heating; full spectrum; photo-thermal synergy

INTRODUCTION

Artificial photosynthesis is the process that can convert carbon dioxide (CO_2) and water (H_2O) into high value-added chemicals (CO, CH_4, CH_3OH, etc.) and oxygen (O_2) with the aid of sunlight and catalysts like semiconductors.[1-3] Rising level of atmospheric CO_2 due to burning fossil fuels caused severe energy and environmental issues, while artificial photosynthesis may address both of them.[4-6] Many work have been done to improve the efficiency of artificial photosynthesis over semiconductors, including crystal facet engineering, element doping/deposition, hetero-structure fabrication, and molecular catalyst modification.[7] However, the low efficiency still impedes its practical applications because classic semiconductor-based solar-to-fuel (STF) processes are struggling in two major trade-off of activity-stability and band edge-redox potential.[4,8] Since it is extremely hard to build the balance, new physics and chemistry are yearned for break-through. In addition, kinetics is usually far less considered than thermodynamics in this process, although the sluggish kinetics of electrochemical CO_2 reduction reaction (CO2RR) and water oxidation reaction, and the reduction half reaction and oxidation half reaction of artificial photosynthesis, respectively, is a common sense.[9,10]

Titanium dioxide (TiO_2) is the most frequently used photocatalyst since 1972, owing to its stability, earth-abundance and non-toxicity. It has been used in many important fields like water cleaning, dye bleaching and pollutant degradation.[11-13] However, TiO_2 is still struggling in STF process

because of its narrow solar spectrum response range (< 400 nm), carriers recombination and sluggish surface reaction kinetics.[14] Recently, coinage metal (Au, Ag and Cu) nanoparticles (NPs) with localized surface plasmon resonance (LSPR) have drawn great attention, as they can absorb wide range of light, especially visible light, by tuning the size, shape and component.[15] They can sensitize wide band gap semiconductors, especially TiO_2, and show considerable visible-light photocatalytic activity in hydrogen evolution reaction (HER), oxygen evolution reaction (OER), and CO2RR through hot electrons and holes.[16-18] Compared to Ag and Cu, Au is the most promising one owing to its suitable LSPR peak position (~550 nm) and oxidation resistance. As a model catalyst, Au/TiO_2 shows promising in practical STF process due to its visible-light response, suitable band position and photo-corrosion resistance, which has been extensively studied and exhibts potential in overall water-splitting (OWS) and artificial photosynthesis.[19,20] The water oxidation reaction sites of Au/rutile plasmonic photocatalysts are studied recently.[21] The Au/rutile can also be used to drive the OWS.[22] Its ability to conduct artificial photosynthesis in continuous flow reactor has been demonstrated,[23] while the STF efficiency is still very low.

Usually it is believed that infrared (IR) cannot be used directly in STF process because its photon energy is too low to drive reduction/oxidation half reactions simultaneously.[8,24] This can lead to a huge loss since IR makes up more than half of the solar spectrum (~54%), resulting in low STF efficiency. However, IR can bring significant thermal effect and temperature increase,[25] which may boost chemical reactions, offering a new approach to take advantage of the full solar spectrum. There are some reports focusing on the heat-enhanced photo (electro)catalytic reaction, although the related mechanism is still under debate. It is reported that electrochemical OWS efficiency can be improved with the help of solar heating,[26] and the photo-thermal catalysis can be realized over Cu7S4@ZIF-8 under 1450 nm laser.[27] However, external heat is usually required in previous work

of thermal-enhanced artificial photosynthesis,[28,29] which is against the initial goal. As a matter of fact, utilization of heating from solar illumination is environmentally friendly and energy saving.

In this work, we demonstrated the Au/rutile photocatalyst can achieve artificial photosynthesis by making utilization of full solar spectrum, among which UV and visible light initiate the reactions, and heat from IR and SPR relaxation boost the reactions. We envision that this may provide novel understanding in full solar spectrum utilization, activation energy of artificial photosynthesis and, specifically, overcoming this activation energy just simply with the help of solar heating.

RESULTS AND DISCUSSION

Structure and Morphology Characteristics

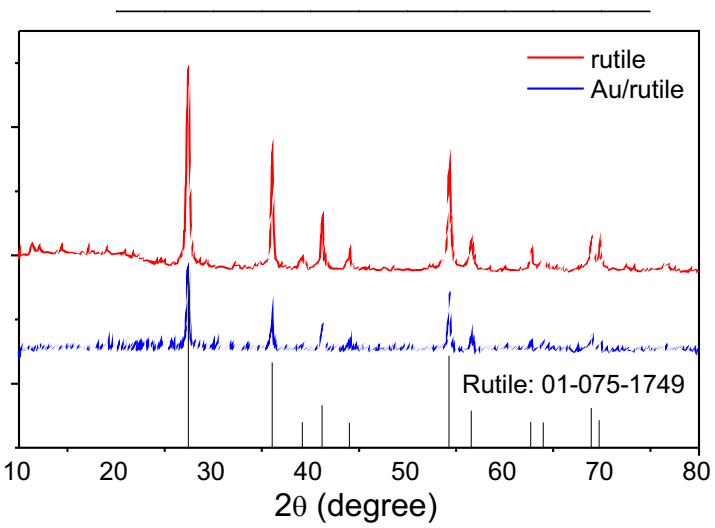

Figure 1. XRD patterns of the rutile and Au/rutile samples.

The Au/rutile samples are chosen as the platform to study the artificial photosynthesis mainly because oxidation half reaction will not become rate limiting step in over-all reaction, as reported previously.[21,22] The crystal structure of the obtained catalysts are studied by the X-ray diffraction

(XRD) technique. The XRD patterns show that the TiO_2 in both samples are in rutile phase (Figure 1), indicating that the Au deposition leads to no change in the crystal phase of TiO_2.

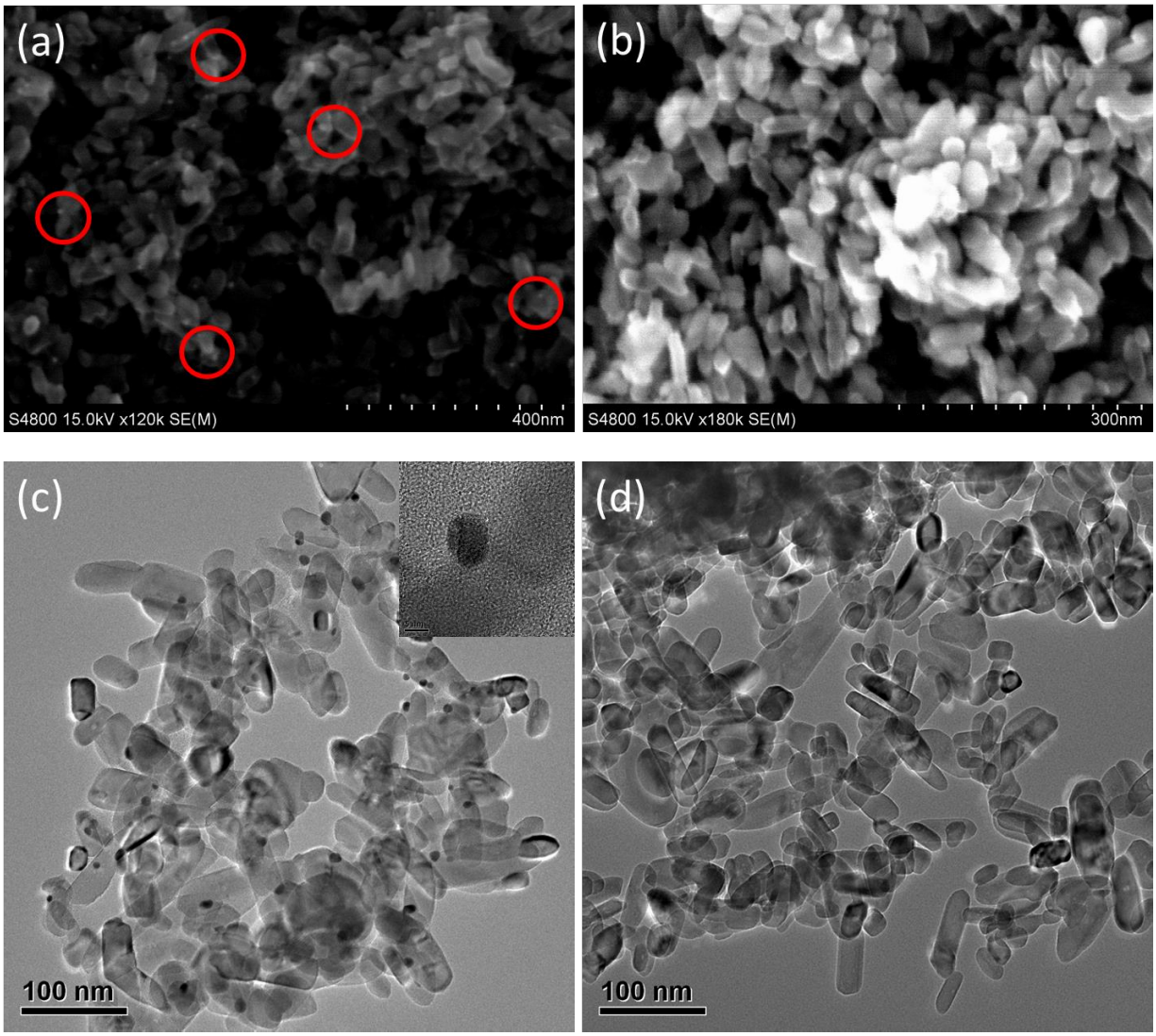

Figure 2. (a,b) SEM and (c,d) TEM images of (a,c) Au/rutile and (b,d) rutile samples. Inset of (c) is the HRTEM image of an Au nanoparticle, for which the scale bar is 5 nm.

Scanning electron microscope (SEM) images show that the obtained rutile are nanoparticles (NPs) with a size around 60 nm (Figures 2a,2b). The scattered bright spots in Figure 2a are Au NPs, which is clearly confirmed by the transmission electron microscope (TEM) images (Figures 2c,2d).

Specifically, the scattered black spots in Figure 2c clearly indicate the presence of Au NPs in the Au/rutile sample, while no such black spots can be observed in the pure rutile sample (Figure 2d). Both TEM and high resolution TEM (HRTEM, inset of Figure 2c) images indicate the size of Au NPs is about 10 nm. The appearance of Au signal in the spectrum collected by energy dispersive X-ray spectroscopy (EDX) can further confirm its existence in Au/rutile (Figure S1), as no Au signal can be observed in the EDX spectrum of rutile sample (Figure S2). All these agree well with the XPS results too (Figures S3-S5). Atomic ratio of Au to Ti in Au/rutile is very low, only about 6.8‰ according to the EDX results. Such a low content of Au in the composite catalyst explains why no diffraction peaks of Au can be observed in the XRD pattern of Au/rutile (Figure 1).

UV-Vis diffuse reflectance spectrum (UV-Vis DRS) shows the typical absorption characteristics of rutile in the UV range (Figure 3), indicating its wide band gap nature with a value of about 3.0 eV derived from the Tauc plot (not shown here). The absorption peak at around 580 nm in the visible range for the Au/rutile sample is caused by the LSPR effect of Au NPs, which is consistent with the aforementioned particle size.[30]

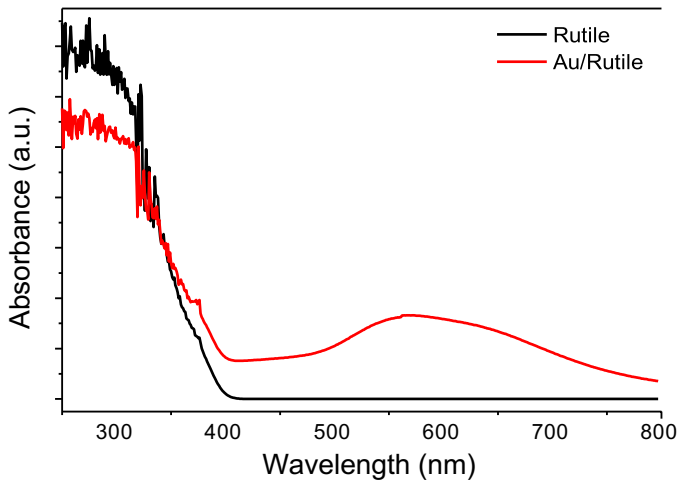

Figure 3. UV-Vis DRS of the rutile and Au/rutile samples.

Catalytic Reduction of CO_2

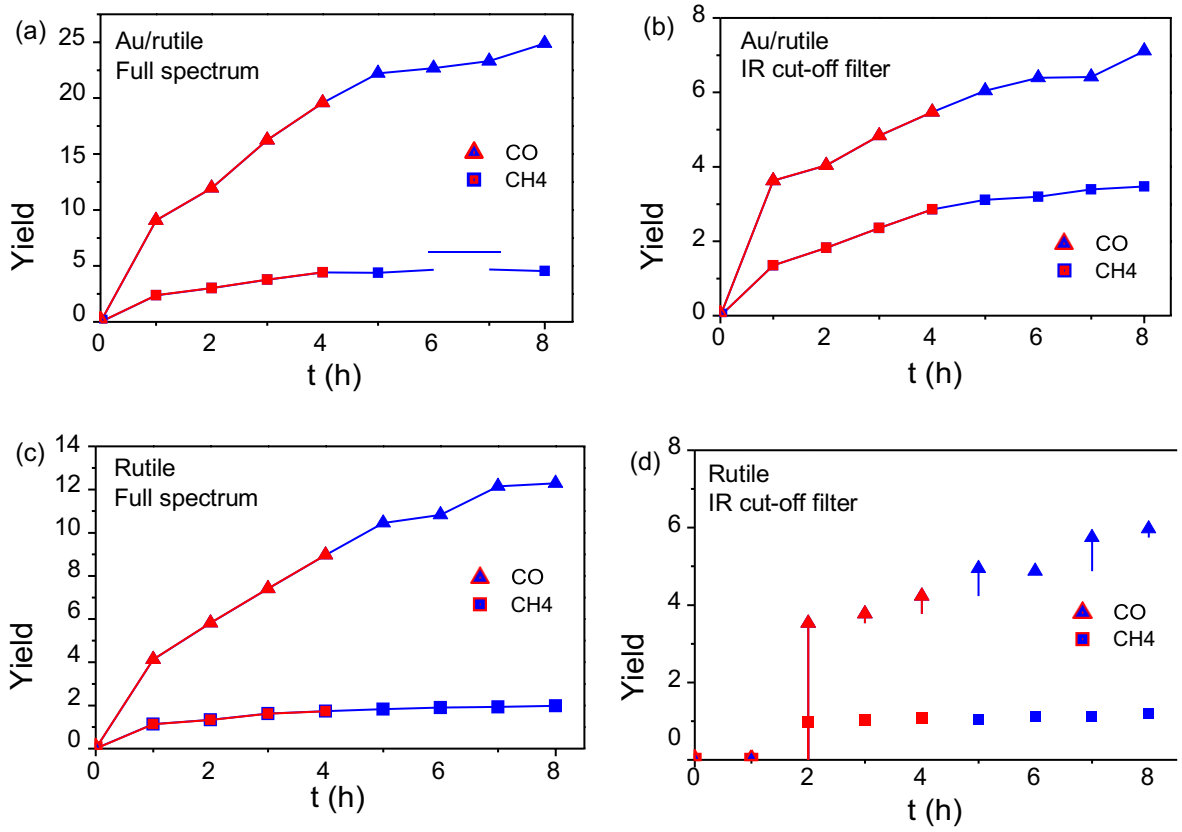

Figure 4. Time *vs* catalytic production of CO and CH_4 over (a,b) Au/rutile and (c,d) rutile catalysts under illumination of (a,c) full spectrum and (b,d) with IR cut-off filter. Blue curves mean that the reactor was cooled down by a circulating-water cooling system, and Red curves refer to that the reactor was not cooled.

CO_2 reduction is used to evaluate the catalytic performance of the obtained Au/rutile and rutile catalysts. No any products were observed in the four control experiments (i.e., blank with and without irradiation, with the catalyst but in dark, and using Ar instead of CO_2 under the same conditions), indicating the CO_2 is indeed the carbon source if a product can be observed. In order to study the solar-heating effect on the catalytic performance, the reactor is not cooled in the first 4 hours and then is cooled down in the next 4 hours. Figure 4a shows catalytic results of CO_2 reduction over Au/rutile catalyst upon full-spectrum irradiation. No H_2 formation is observed for

both cases, either because no H_2 is formed or the produced amount is beyond our GC detection limit. Furthermore, CO and CH_4 are the major products in both cases. Clearly, the formation rate (μmol/g/h) of both CO (r_{CO}) and CH_4 (r_{CH4}) slows down once the reactor is cooled. The CO_2 reduction is also carried out with an IR cut-off filter (> 860 nm), whereas light intensity in the UV-visible range is kept nearly unchanged (Figure 4b), so as to figure out the solar-heating effect on the catalytic reduction of CO_2. The catalytic performance becomes much lower compared to those under full-spectrum illumination, while the one without being cooled is still higher than that being cooled. That is to say, the Au/rutile catalyst exhibits enhanced activity for the reaction system without being cooled, no matter it is under UV-visible light or full-spectrum illumination. So such enhancement may not be specifically caused by the Au/rutile catalyst.

Obviously, CO2RR or OER cannot be activated by IR-light irradiation over the Au/rutile catalyst, let alone the CO2RR and OER be activated simultaneously,[8,24] as no light can be absorbed in this case. In other words, one cannot use the processes related to the classic photo-generated electron-hole pairs to explain the decrease in activity when the reaction system is cooled down.[31] Unlike some materials with up-conversion property,[32] what is reported here is thus not a direct IR-induced STF process. It is noted that the final temperature of aqueous solution after illumination with full-spectrum light is the highest (~333 K), followed by the one with IR cut-off filter (~303 K), and the one being cooled is the lowest (~288 K). Such an order is the same as that of the catalytic activity. Since the temperature increase caused by the solar heating is on a case by case basis, it is believed that the observed enhancement phenomena in this work are mainly temperature dependent.

To further confirm that the catalytic activity is temperature dependent, the catalytic performance was investigated using pure rutile catalyst under the same experimental conditions (Figures 4c,4d). As reported previously,[20] pure rutile shows inferior r_{CO} and r_{CH4} to Au/rutile due to the hot electron

reduction, lower charge separation and/or less active sites. Albeit a higher temperature is observed for the Au/rutile system (~333 K) than the rutile one (~328 K) due to the relaxation of Au LSPR, the order of catalytic activity is still consistent with that of the temperature, i.e., full spectrum > IR filter (~298 K) > being cooled (~288 K). Since the CO_2 photoreduction can be realized over both rutile under UV-light illumination[33] and Au/rutile under either UV or visible light irradiation,[34] it is believed that the CO_2 reduction can indeed be boosted by solar thermal effect.

In addition, considering the amount of Au NPs in the Au/rutile system is very low (0.2 mg of Au, 20 mg of rutile and 15 g of H_2O), the relative small increase amplitude in the temperature (~5 K) due to the presence of Au NPs cannot be ignored, mainly because it can still influence the catalytic activity greatly. As indicated in Figure 4, the Au/rutile system exhibits a much larger r_{CO} and r_{CH4} than pure rutile in almost all the experiments carried out in this work, with the exception of r_{CO} using an IR cut-off filter, for which the Au/rutile shows a slightly larger r_{CO} than rutile. This means that the thermal effect induced by Au LSPR is considerably significant for the catalytic reduction of CO_2. As a matter of fact, a giant temperature increase (over 500 K) on nano-sized Au upon illumination has been reported both experimentally and theoretically.[35]

Furthermore, an interesting phenomenon is observed when a specific temperature is acquired by an external heating source instead of the IR light. That is to say, the catalytic reduction of CO_2 boosted by solar heating under full-spectrum irradiation without being cooled is compared to that by water-bath heating at the same temperature but with IR cut-off filter (Figure 5). It is found that at the same temperature the catalytic activity using solar heating is much higher than that using water-bath heating for the CO production over both rutile and Au/rutile catalysts as well as for the CH_4 evolution over rutile; whereas the CH_4 evolution shows an opposite rule over Au/rutile. This is ascribed to the photo-thermal synergy, as reported previously.[36] In the presence of Au NPs, in

addition, the observed temperature may not be the 'real' one adjacent to the catalysts due to the local heating effect of plasmonic metal NPs.[35] This can also lead to the aforementioned difference in the catalytic activity of CO_2 reduction.

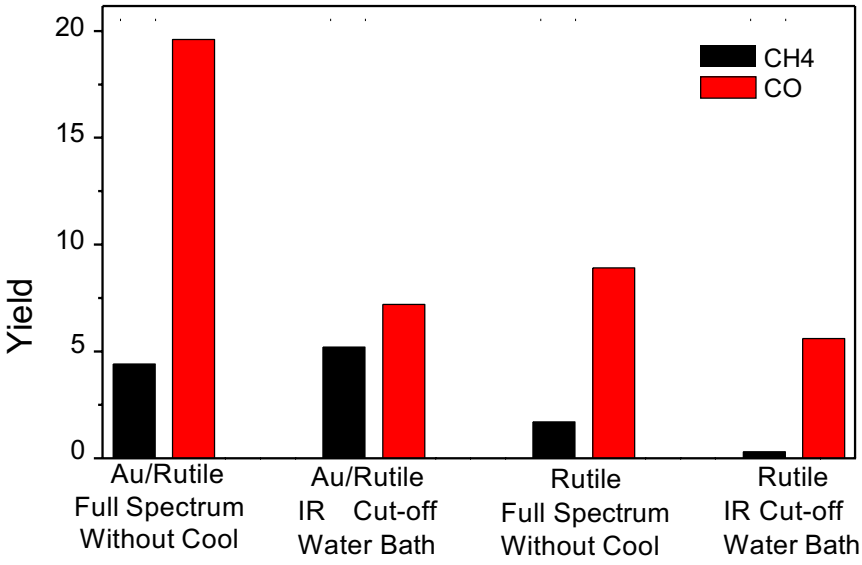

Figure 5. Comparing the catalytic activity boosted by solar heating to that by water-bath heating.

Apparent Activation Energy and Kinetic Concern

Apparent activation energy (*E*a) of CO and CH_4 formation reaction is determined using Ahrrenius equation so as to study the related kinetics (Supporting Information). Thus, the catalytic reduction of CO_2 over Au/rutile and rutile catalysts is done with IR cut-off filter at different temperatures (Figure 6). Clearly, both the r_{CO} and r_{CH4} increase with elevating temperature. The *E*a of CH_4 formation reaction (Ea_{CH4}) is about 17.3 kJ/mol using Au/rutile, higher than 5.5 kJ/mol of Ea_{CO}. This explains well kinetically the inferior r_{CH4} to r_{CO}, although the formation of CH_4 is more thermodynamically favorable than that of CO. Albeit the sluggish kinetics of CO2RR is a common

sense for a long time,[4,7,8] only recently few work has related the reaction kinetics to the catalytic performance[37,38] and in most cases the thermodynamics (CB position or flat-band potential vs. standard redox potential) is still the major concern.[39] The difference between Ea_{CH4} and Ea_{CO} may be closely related to the multiple proton-coupled-electron-transfer (PCET) process involved in the CO_2 reduction.[40] More electrons and protons are involved in the CH_4 formation than those for CO production. As predicted by the classic collision theory,[41] such proton-involved process can be enhanced greatly with increasing temperature. Moreover, the kinetic resistance of multiple PCET process at room temperature has been reported.[42]

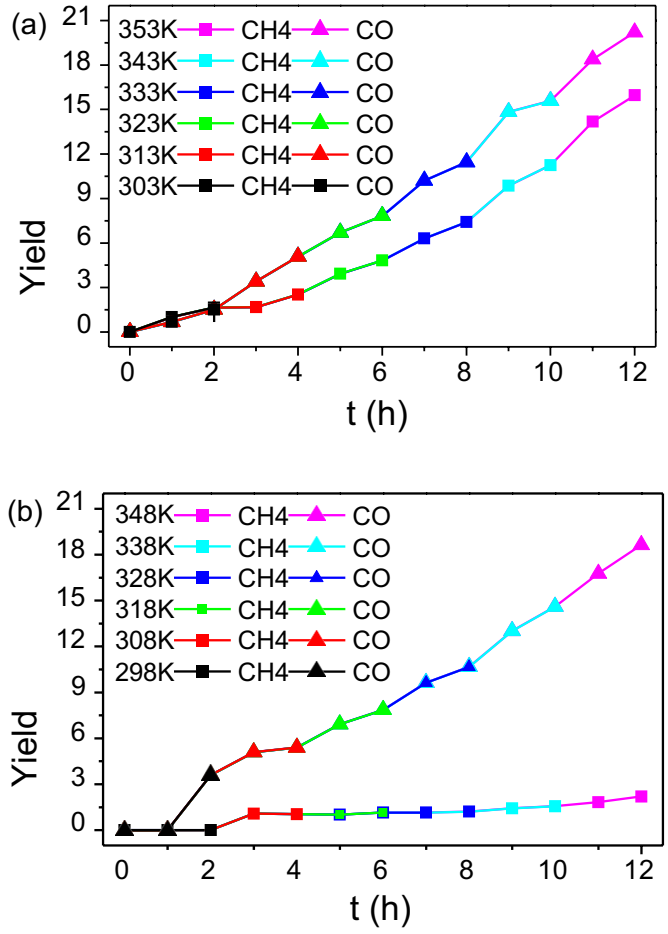

Figure 6. Time *vs* CO and CH_4 production yield at different temperatures for (a) Au/rutile and (b) rutile.

Similarly, the Ea_{CH4} and Ea_{CO} using pure rutile catalyst are calculated to be 77.5 and 35.6 kJ/mol, respectively (Supporting Information). Like that using Au/rutile, the Ea_{CH4} using the rutile is still higher than Ea_{CO}. Interestingly, both of them are much larger than those using Au/rutile. Besides the commonly used visible-light harvesting, charge separation and/or hot-electron injection,[43] this provides the kinetic explanation about the superior catalytic performance of Au/rutile to pure rutile. It is noted that direct experimental evidence that the co-catalyst can lower the activation energy of catalytic CO2RR is rarely provided, although it is reported that the reaction pathways of electro-CO2RR can be altered by a co-catalyst like Au.[44] Thus, herein we correlate the enhanced catalytic activity of CO_2 reduction for the first time to the kinetics based on the calculated *Ea* results when plasmonic Au NPs are introduced into the catalytic system.

To further verify the above conclusion that the PCET process in CO_2 reduction is kinetics related, the catalytic experiments are conducted by changing CO_2 partial pressure (P_{CO2}). The catalytic activity over Au/rutile under full-spectrum illumination at 'unit' pressure of ~108 kPa is compared to that under half-'unit' pressure of ~54 kPa (balanced by Ar). Figure 7 shows the 4-h catalytic yield of CO and CH_4. The r_{CO} over Au/rutile is slowed down greatly when reducing P_{CO2}, while the r_{CH4} is just slightly changed (Figure 7a). This means that r_{CO} is more sensitive to P_{CO2} than r_{CH4}, possibly implying that the r_{CH4} is more restricted by the post-transfer steps like PCET, instead of by the reactants-involved steps like adsorption and/or photochemical transformation, and vice versa for CO. However, such sensitivity becomes less evident for the rutile catalyst (Figure 7b). Moreover, the r_{CO} over rutile slightly increases when reducing P_{CO2}. This may be because the whole reaction over rutile is limited by the OER, instead of CO2RR-related steps, due to the poor water oxidation capability.[21]

Therefore, it is suggested that the kinetics can play a crucial role in the activity and selectivity of CO_2 reduction. In all cases, the r_{CO} is higher than r_{CH4} owing to its low *E*a. Due to the same reason, as manifested in Figure 4, the production yield of CO increases more greatly with elevating temperature than that of CH_4, no matter the catalyst is rutile or Au/rutile. In addition, a higher r_{CH4} at elevated temperature is ascribed to the acceleration of post-transfer steps (i.e., PCET), like the classic temperature-dependent chemical reaction; while the enhanced r_{CO} is related to both the *E*a and CO desorption. Although CO exhibits a strong binding energy to Au NPs,[45] elevating the temperature can promote its desorption and, thereby, improving the catalytic activity.

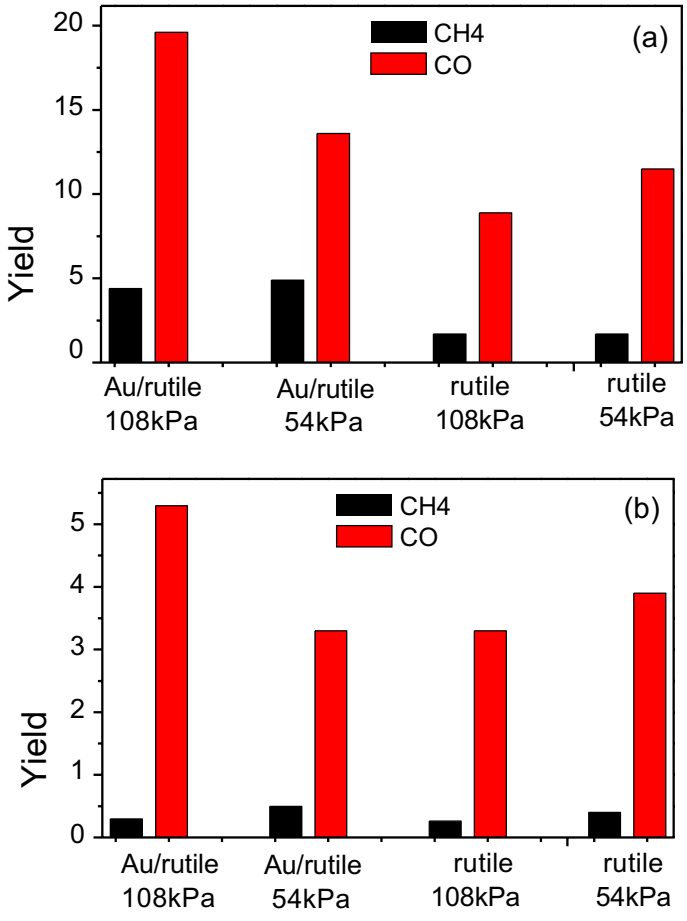

Figure 7. P_{CO2} related photocatalytic activity over Au/rutile and rutile catalysts after 4-h reaction with the reactor (a) not being cooled and (b) being cooled.

It is known that the photocatalysis is commonly carried out at ambient temperature. The *E*a is the core concept of reaction kinetics and catalysis, specifically in traditional thermal catalysis,[36] which indicates the dependence of reaction rate on the temperature. However, in most cases the *E*a and reaction kinetics are usually overlooked in photocatalysis, which may lead to incomplete, or even wrong, elucidation of the reaction mechanism. Only recently *E*a is once again attracting concern to study the temperature-dependent reaction rate, especially in the SPR-based photocatalysis since the thermal effect induced by the SPR relaxation cannot be ignored;[46,47] while most of them are about the 'down-hill' reactions rather than the 'up-hill' ones. Like many other chemical reactions, the catalytic reduction of CO_2 also follows the classic Ahrrenius temperature-dependent reaction rate. So a high collision frequency between the molecules and catalysts is expected.[41] With this regard, solar heating can be used to overcome the reaction activation energy, providing a simple approach compared to the others like prolonging the lifetime of key intermediates via surface-engineering.[48] Accordingly, there may be no need to cool down the reactor during photocatalytic reduction of CO_2, as demonstrated above. Meanwhile, the utilization of plasmonic metal NPs can lead to strong photo-thermal synergetic effect, which further improves the catalytic performance. It is also noted that the different *E*a comes not only from CO2RR on Au/rutile, but also from easier OER kinetics brought by the metal-oxide interface.[21] The sluggish kinetics can thus be speeded up, and the traditional trade-off in semiconductor-based photocatalytic reactions may be avoided.[8]

Furthermore, full solar spectrum (UV, visible and IR light) can be simultaneously utilized in such a catalytic system. All these can be in favor of future real applications, not only for the cost concern, but also the STF efficiency.

Conclusion

In summary, we have demonstrated that Au NPs deposited rutile can realize catalytic reduction of CO_2 via utilizing full solar spectrum. The UV and visible light can activate the reaction (i.e., thermodynamically), and the heat from IR light as well as photo-thermal effect from SPR can boost the reaction (i.e., kinetically). This is in favor of the utilization of solar energy, especially the IR light with low photon energy. Moreover, the mechanism of enhanced production yield of CO and CH_4 over Au/rutile catalyst has been investigated from the kinetic point of view based on the study of apparent activation energy experimentally, which plays a critical role in the STF process. So the plasmonic system can be a promising catalyst in practical artificial photosynthesis, specifically for full-solar spectrum utilization, in case SPR utilization efficiency is high enough in future.

Materials and Methods

Catalysts preparation

Commercial rutile (Aladin) was used as the model catalyst. Au NPs were deposited onto the rutile (denoted as Au/rutile) using a similar protocol reported previously, in which the mechanism and active sites of water oxidation reaction driven by hot holes on Au/rutile were clearly elucidated,[21] as well as the OWS.[22] Au/rutile is a suitable platform to study artificial photosynthesis because oxidation half reaction will not become rate-limiting step in the over-all reaction.

Materials characterization

The crystal structure of as-prepared products was investigated by X-ray diffraction (XRD) using Bruker D8 focus diffractometer with Ni-filtered Cu-Kα radiation. The diffractograms were collected in the 2θ range of 10–80°at a scan rate of 0.1°/min. UV –Vis diffuse reflectance spectra (UV–vis DRS) were recorded with the wavelength ranging from 250 to 800 nm on Lambda 750 UV/visible/NIR spectrophotometer using $BaSO_4$ as the reference. Morphology and composition

of the obtained samples were analyzed by using Hitachi S4800 field-emission scanning electron microscopy (SEM) equipped with energy dispersive X-ray spectrometer (EDX) and Tecnai G2 F20 U-TWIN transmission electron microscopy (TEM).

Photocatalytic evaluation

Catalytic reduction of CO_2 was carried out using the photoreaction system described previously.[49] Typically, 20 mg of catalyst was used. High purity CO_2 gas (≥ 99.999%) was first bubbled before the reaction in a quartz reactor containing 15 mL of aqueous catalyst suspension. The wet CO_2 was flown through the whole system for ~40 min to ensure complete removal of air from the system and maximum adsorption of CO_2 molecules onto the active sites of the catalyst. A positive pressure of 25 kPa was maintained inside the system. A 300-W xenon lamp was placed 14-15 cm above the upper surface of the suspension. The system was constantly recycled with tap water (15 ℃) during the entire reaction using water recycling pump. The reactor could be cooled down in the same system when necessary. The products were detected using He as the carrier gas by 7890A GC/LC system (Agilent) equipped with two (front and back) flame ionization detectors (FID) and one thermal conductivity detector (TCD) via an automated gas valve. Four control experiments were performed to study whether or not the observed products were from the CO_2 reduction, i.e., blank reactor with and without irradiation, dark experiment with the catalyst, and using Ar instead of CO_2 under the same experimental conditions.

Associated Content:

Supporting Information.

All supporting information are available free of charge via the Internet at http://pubs.acs.org, including EDX and XPS spectra of Au/rutile and rutile, and calculation of *E*a.

AUTHOR INFORMATION

Corresponding Author

* Tao He, E-mail: het@nanoctr.cn

ORCID

Tao He: 0000-0001-6336-2402.

Notes

The authors declare no competing financial interest.

Acknowledgements:

This work was supported by the Belt and Road Initiative by Chinese Academy of Sciences.

References:

1. Gust, D.; Moore, T. A.; Moore, A. L. Solar fuels via artificial photosynthesis. *Acc. Chem. Res.* **2009***, 42*, 1890-1898.
2. Nocera, D. G. The artificial leaf. *Acc. Chem. Res*. **2012**, *45*, 767-776.
3. Morris, A. J.; Meyer, G. J.; Fujita, E. Molecular approaches to the photocatalytic reduction of carbon dioxide for solar fuels. *Acc. Chem. Res.* **2009**, *42*, 1983-1994.
4. Tu, W.; Zhou, Y.; Zou, Z.G. Photocatalytic conversion of CO_2 into renewable hydrocarbon fuels: State-of-the-art accomplishment, challenges, and prospects. *Adv. Mater.* **2014**, *26*, 4607-4626.
5. Maginn, E. J. What to do with CO_2. *J. Phys. Chem. Lett.* **2013**, *1*, 3478-3479.
6. Aresta, M.; Dibenedetto, A.; Aresta, M.; Dibenedetto, A. Utilisation of CO_2 as a chemical feedstock: Opportunities and challenges. *Dalton Transact.* **2007**, *28*, 2975-2992.
7. White, J. L.; Baruch, M. F.; Pander, J. E.; Hu, Y.; Fortmeyer, I. C.; Park, J. E.; Zhang, T.; Liao, K.; Gu, J.; Yan, Y.; Shaw, T. W.; Abelev, E.; Bocarsly, A. B. Light-driven heterogeneous reduction of carbon dioxide: Photocatalysts and photoelectrodes. *Chem. Rev.* **2015**, *115*, 12888-12935.

8. Habisreutinger S. N.; Schmidt‐Mende L.; Stolarczyk J. K. Photocatalytic reduction of CO_2 on TiO_2 and other semiconductors. *Angew. Chem. Int. Ed.* **2013**, *52*, 7372-7408.

9. Ran, J.; Jaroniec, M.; Qiao, S. Z. Cocatalysts in semiconductor-based photocatalytic CO_2 reduction: Achievements, challenges, and opportunities. *Adv. Mater.* **2018**, *30*, 17046-17049.

10. Strickler, A. L.; Escudero, M.; Jaramillo, T. F. Core–shell Au@metal-oxide nanoparticle electrocatalysts for enhanced oxygen evolution. *Nano Lett.* **2017** *17*, 6040-6046.

11. Low, J.; Cheng, B.; Yu, J. Surface modification and enhanced photocatalytic CO_2 reduction performance of TiO_2: A review. *Appl. Surf. Sci.* **2017**, *392*, 658-686.

12. Inoue, T.; Fujishima, A.; Konishi, S.; Honda, K. Photoelectrocatalytic reduction of carbon dioxide in aqueous suspensions of semiconductor powders. *Nature* **1979**, *277,* 637-638.

13. Wang M.; Iocozzia J.; Sun L.; Lin, C.; Lin, Z. Inorganic-modified semiconductor TiO_2 nanotube arrays for photocatalysis. *Energy Environ. Sci.* **2017**, *7*, 2182-2202.

14. Ma, Y.; Wang, X.; Jia, Y.; Chen, X.; Han, H.; Li, C. Titanium dioxide-based nanomaterials for photocatalytic fuel generations. *Chem. Rev.* **2014**, *114*, 9987-10043.

15. Hartland, G. V.; Besteiro, L. V.; Johns, P.; Govorov, A. O. What's so hot about electrons in metal nanoparticles? *ACS Energy Lett.* **2017**, *2*, 1641-1653.

16. Lou, Z.; Kim, S.; Zhang, P.; Shi, X.; Fujitsuka, M.; Majima, T. In-situ observation of single Au triangular nanoprism etching to various shapes for plasmonic photocatalytic hydrogen generation. *ACS Nano* **2016**, *11*, 968-974.

17. Yu, S.; Wilson, A. J.; Kumari, G.; Zhang, X.; Jain, P. K. Opportunities and challenges of solar-energy-driven carbon dioxide to fuel conversion with plasmonic catalysts. *ACS Energy Lett.* **2017**, *2*, 2058-2070.

18. Naldoni, A.; Montini, T.; Malara, F.; Mróz, M. M.; Beltram, A.; Virgili, T.; Boldrini, C. L.; Marelli, M.; Romero-Ocaña, I.; Delgado, J. J.; Danto V. D.; Fornasiero, P. Hot electron collection on brookite nanorods lateral facets for plasmon-enhanced water oxidation. *ACS Catal.* **2017**, *7,* 1270-1278.

19. Zhang, J.; Jin, X.; Morales-Guzman, P. I.; Yu, X.; Liu, H.; Zhang, H.; Razzari, L.; Claverie, J. P. Engineering the absorption and field enhancement properties of Au-TiO_2 nanohybrids via whispering gallery mode resonances for photocatalytic water splitting. *ACS Nano* **2016,** *10*, 4496-4503.

20. Hou, W.; Wei, H. H.; Pavaskar, P.; Goeppert, A.; Aykol, M.; Cronin, S. B. Photocatalytic conversion of CO_2 to hydrocarbon fuels via plasmon-enhanced absorption and metallic interband transitions. *ACS Catal.* **2011**, *1*, 929-936.

21. Wang, S.Y.; Gao, Y.Y.; Miao, S.; Liu, T.F.; Mu, L.C.; Li, R.G.; Fan, F.T.; Li, C. Positioning the water oxidation reaction sites in plasmonic photocatalysts. *J. Am. Chem. Soc.* **2017**, *139*, 11771-11778.

22. Wang, S.Y.; Gao, Y.Y.; Qi, Y.; Li, A. L.; Fan, .F.T.; Li, C. Achieving overall water splitting on plasmon-based solid Z-scheme photocatalysts free of redox mediators. *J. Catal*. **2017**, *354*, 250-257.

23. Rechberger, F.; Niederberger, M. Translucent nanoparticle-based aerogel monoliths as 3-dimensional photocatalysts for the selective photoreduction of CO_2 to methanol in a continuous flow reactor. *Mater. Horizons* **2017**, *4*, 1115-1121.

24. Kim W.; Edri E.; Frei H. Hierarchical inorganic assemblies for artificial photosynthesis. *Acc. Chem. Res.* **2016**, *49*, 1634-1645.

25. Gan, Z.; Wu, X.; Meng, M.; Zhu, X.; Yang, L.; Chu, P. K. Photothermal contribution to enhanced photocatalytic performance of graphene-based nanocomposites. *ACS Nano* **2014**, *8*, 9304-9310.

26. Wang, J.; Zhu, L.; Dharan, G.; Ho, G. W. Electrodeposited cobalt phosphide superstructures for solar-driven thermoelectrocatalytic overall water splitting. *J. Mater. Chem. A* **2017***, 5,* 16580-16584.

27. Wang, F.; Huang, Y.; Chai, Z.; Zeng, M.; Li, Q.; Wang, Y.; Xu, D. S. Photothermal-enhanced catalysis in core–shell plasmonic hierarchical Cu_7S_4 microsphere@zeolitic imidazole framework-8. *Chem. Sci.* **2016**, *7*, 6887-6893.

28. Dilla, M.; Mateblowski, A.; Ristig, S.; Strunk, J. Photocatalytic CO_2 reduction under continuous flow high-purity conditions: Influence of light intensity and H_2O concentration. *ChemCatChem* **2017**, *9*, 4303-4303.

29. Zhang, L.; Kong, G.; Meng, Y.; Tian, J.; Zhang, L.; Wan, S.; Lin J. D.; Wang Y. Direct coupling of thermo- and photocatalysis for conversion of CO_2-H_2O to fuels. *ChemSusChem* **2017**,*10,* 4709-4714.

30. Zhou, M.; Zeng, C.; Chen, Y.; Zhao, S.; Sfeir, M. Y.; Zhu, M. Z.; Jin R. C. Evolution from the plasmon to exciton state in ligand-protected atomically precise gold nanoparticles. *Nature Comm.* **2016**, *7*, 13240-13246.

31. Wang, F.; Li, Q.; Xu, D. S. Recent progress in semiconductor-based nanocomposite photocatalysts for solar-to-chemical energy conversion. *Adv. Energy Mater.* **2017**, *7*, 1700529.

32. Majek, M.; Faltermeier, U.; Dick, B.; Pérezruiz, R.; Jacobi, V. W. A. Application of visible- to-UV photon upconversion to photoredox catalysis: The activation of aryl bromides. *Chemistry* **2015**, *21*, 15496-15501.

33. Liu, L. J.; Zhao, H. L.; Andino, J. M.; Li, Y. Photocatalytic CO_2 reduction with H_2O on TiO_2 nanocrystals: Comparison of anatase, rutile, and brookite polymorphs and exploration of surface chemistry. *ACS Catal.* **2012**, *2*, 1817-1828.

34. Maruo, Y. Y.; Sasaki, M.; Hino, S.; Sato, A. Effect of TiO_2 crystal structure on CO_2 photoreduction using Au nanoparticles on TiO_2 catalyst. *IEEE International Conference on Nanotechnology* **2016**.

35. Agarwal, D.; Aspetti, C. O.; Cargnello, M.; Ren, M. L.; Yoo, J.; Murray, C. B.; Agarwal, R. Engineering localized surface plasmon interactions in gold by silicon nanowire for enhanced heating and photocatalysis. *Nano Lett.* **2017**, *17,* 1839-1845.

36. Santen, R. A.; Neurock, M.; Shetty, S. G. Reactivity theory of transition-metal surface: A Bronsted-Evans-Polanyi linear activation energy-free energy analysis. *Chem. Rev.* **2010**, *110*, 2005-2048.

37. Jiang H.; Hou Z.; Luo Y. Unraveling the mechanism for the sharp-tip enhanced electrocatalytic carbon dioxide reduction: the kinetic decides. *Angew. Chem. Int. Ed.* **2017**, *56*, 15617-15621.

38. Liu, M.; Pang, Y.; Zhang, B.; De, L. P.; Voznyy, O., Xu, J. X.; Zheng, X. L.; Dinh, C. T.; Fan, F. J.; Cao, C. H.; Arquer, F. P.; Safaei, T. S.; Mepham, A.; Klinkova, A.; Kumacheva, E.; Filleter, T.; Sinton, D.; Kelly, S. O.; Sargent, E. H. Enhanced electrocatalytic CO_2 reduction via field-induced reagent concentration. *Nature* **2016**, *537,* 382–386.

39. Luo, Y.; Li, G.; Zhang, X.; Xin, B.; Shi, G. D.; Li Y.; Wong, P. K.; Yu, J. C.; Yu, Y. Enhanced activity and stability of carbon-decorated cuprous oxide mesoporous nanorods for CO_2 reduction in artificial photosynthesis. *ACS Catal.* **2016**, *6*, 6444–6454.

40. Warren, J. J.; Tronic, T. A.; Mayer, J. M. The thermochemistry of proton-coupled electron transfer reagents and its implications. *Chem. Rev.* **2010**, *110*, 6961-7001.

41. Prigogine, I. *Adv. Chem. Phys.* Volume 5. John Wiley & Sons, Inc. **2007**, 353.

42. Indrakanti, V. P.; Kubicki, J. D.; Schobert, H. H. Photoinduced activation of CO_2 on Ti-based heterogeneous catalysts: Current state, chemical physics-based insights and outlook. *Energy Environ. Sci.* **2009**, *2*, 745-758.

43. Hou, W.; Cronin, S. B. A review of surface plasmon resonance-enhanced photocatalysis. *Adv. Func. Mater.* **2013**, *23*, 1612-1619.

44. Peterson, A. A.; Nørskov, J. K. Activity descriptors for CO_2 electroreduction to methane on transition-metal catalysts. *J. Phy. Chem. Lett.* **2012**, *3,* 251-258.

45. Meier, D. C.; Goodman, D. W. The influence of metal cluster size on adsorption energies: CO adsorbed on Au clusters supported on TiO_2. *J. Am. Chem. Soc.* **2004**, *126*, 1892-1899.

46. Nishi, H.; Tatsuma, T. Oxidation ability of plasmon-induced charge separation evaluated on the basis of surface hydroxylation of gold nanoparticles. *Angew. Chem. Int. Ed.* **2016**, *55*, 10771-10775.

47. Zhou, L. N.; Swearer, D. F.; Zhang, C.; Robatjazi, H.; Zhao, H. Q.; Henderson, L.; Dong, L. L.; Christopher, P.; Carter, E. A.; Nordlander, P.; Halas, N. J. Quantifying hot carriers and thermal contributions in plasmonic photocatalysis. *Science* **2018**, *362*, 69-72.

48. Liang, L.; Lei, F.; Gao, S.; Sun, Y. F.; Jiao, X. C.; Wu, J.; Qamar, S.; Xie, Y. Single unit cell bismuth tungstate layers realizing robust solar CO_2 reduction to methanol. *Angew. Chem. Int. Ed.* **2015**, *54*, 13971-13974.

49. Ehsan, M. F.; He, T. In situ synthesis of ZnO/ZnTe common cation heterostructure and its visible-light photocatalytic reduction of CO_2 into CH_4. *Appl. Catal. B* **2015**, *166-167*, 345-352.

TOC

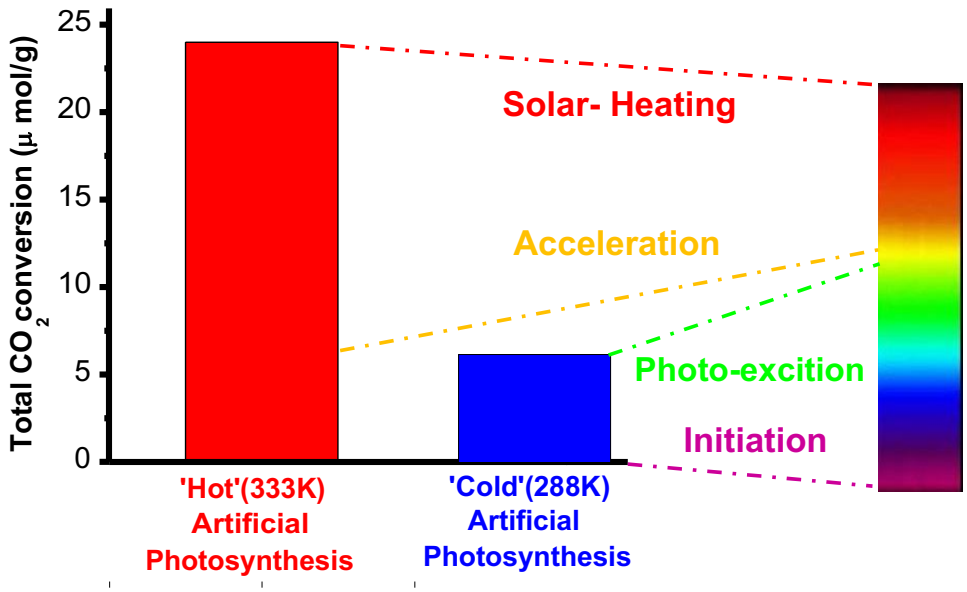
Total CO2 conversion (μ mol/g)
25
20
15
10
5
0
Solar- Heating
Acceleration
Photo-excition
Initiation
'Hot'(333K)
Artificial
Photosynthesis
'Cold'(288K)
Artificial
Photosynthesis